Available online at www.sciencedirect.com

ScienceDirect

Procedia Engineering 63 (2013) 397 – 404

Procedia Engineering

www.elsevier.com/locate/procedia

The Manufacturing Engineering Society International Conference, MESIC 2013

Comparison of Ti-5Al-5V-5Mo-3Cr Welds Performed by Laser Beam, Electron Beam and Gas Tungsten Arc Welding

T. Pasang[a,]*, J.M.Sánchez Amaya[b], Y. Tao[a], M.R. Amaya-Vazquez[b], F.J. Botana[b], J.C Sabol[c], W.Z. Misiolek[c], O. Kamiya[d]

[a]*Dept. of Mechanical Eng., AUT University, Auckland 1020, New Zealand*

[b]*Universidad de Cádiz. Departamento de Ciencia de los Materiales e Ingeniería Metalúrgica y Química Inorgánica. Avda. República Saharaui s/n, 11510-Puerto Real, Cádiz, Spain*

[c]*Institute for Metal Forming, Lehigh University, 5 East Packer Avenue, Bethlehem, PA 18015, USA*

[d]*Department of Mechanical Engineering, Akita University, Akita City, Japan*

Abstract

Welding characteristics of Ti-5Al-5V-5Mo-3Cr (Ti5553) alloy has been investigated. The weld joints were performed by laser beam (LBW), electron beam (EBW) and gas tungsten arc welding (GTAW). Regardless of the welding method used, the welds showed low hardness values with coarse columnar grains in the fusion zone (FZ) and retained equiaxed beta phase within the heat affected zone (HAZ). Larger grains were present at the near HAZ compared with far HAZ (near base metal). The strengths of the welded samples were lower than the base metal. Fracture occurred at the weld zones with transgranular and microvoid coalescence fracture mechanism.

Selection and peer-review under responsibility of Universidad de Zaragoza, Dpto Ing Diseño y Fabricacion

Keywords: Laser beam welding; electron beam welding; tungsten inert gas welding; titanium alloys; Ti-5Al-5V-5Mo-3Cr

* Corresponding author. Tel.: +64-9-921 9999 ext. 8760; fax: +64-9-921 9999.
E-mail address: tpasang@aut.ac.nz

Selection and peer-review under responsibility of Universidad de Zaragoza, Dpto Ing Diseño y Fabricacion
doi:10.1016/j.proeng.2013.08.202

1. Introduction

It is generally known that commercially pure titanium, α-titanium and α/ β titanium have excellent weldability. Metastable β titanium alloys, however, may have limited weldability due to the high content of β stabilizing elements [Donachie, 2000]. Some of the weldability studies on metastable β titanium are summarized in the following. In general, in the as-welded (AW) condition the weld fusion zone (FZ) is comprised of coarse columnar β grains from solidification while the heat affected zone (HAZ) adjacent to the fusion lines are characterized by retained β structure. In this condition, they are low in strength (low hardness) but have good ductility. Becker and Baeslack (1980) conducted weldability studies on three different types of metastable β titanium alloys (Ti-15V-3Cr-3Al-3Sn; Ti-8V-7Cr-3Al-4Sn-1Zr and Ti-8V-4Cr-2Mo-2Fe-3Al) and showed that the alloys are readily weldable. Their findings confirmed the above explanations. For all three alloys, the strengths were increased with post weld heat treatment at, however, the expense of ductility. Weldability of Beta-21S sheet using laser welding technique was investigated by Liu at al. (1993). Both the FZ and HAZ were narrow with fine retained β grain structure. The FZ had a "crown-shaped" (more literatures refer to as an hour glass-shaped, hence, used in this paper) with wider top and bottom surfaces compared with the mid-thickness area. Epitaxial grain growth was observed to form from the narrow HAZ through the fusion boundary into the FZ. The FZ had a transitioned from a solidification mode of a cellular-type along the fusion boundary to a complete cellular-dendritic (or columnar dendritic) solidification mode at the weld centreline. Baeslack et al. (1993a) conducted welding investigations on Beta-C^{TM} implementing gas tungsten arc welding (GTAW or TIG). The as-welded samples showed epitaxial growth from the near-HAZ into the FZ, solidified with a cellular mode and progressively formed a complete columnar-dendritic grain structure at the weld centreline.

In the early 2000s, a new metastable β titanium alloy known as Ti-5Al-5V-5Mo-3Cr (Ti5553) was introduced. Apart from its high strength, excellent hardenability and fracture toughness, it also offers high fatigue resistance. The potential applications of this alloy are in the high-strength related areas such as landing gear and pylon/nacelle areas. Note that the landing gear beam truck of Boeing 787 has been successfully manufactured using this alloy (Fanning and Boyer, 2003). To find more applications in different areas, a number of factors are to be investigated, and one of them is the weldability. According to Donachie (2000), Leyens and Peters (2003), the most common welding techniques to joint titanium and its alloys are GTAW, gas metal arc welding (GMAW/MIG), plasma arc welding (PAW), laser beam welding (LBW) and electron beam welding (EBW). The first three methods fall in the arc welding category with high heat input and low power density of heat source, while the last two techniques belong to high-energy beam group.

This paper presents findings from a recent investigation with the objective of comparing the microstructures and properties of the Ti5553 welds following different types of welding methods. Three of the above five methods were employed, i.e. LBW, EBW and GTAW.

2. Experimental Procedures

2.1. Materials

The alloy used in this investigation was provided by the Boeing Aircraft Company, and that is a new metastable β titanium, Ti-5Al-5V-5Mo-3Cr (Ti5553). The alloy was in the annealed condition with a typical α/β microstructure. The chemical composition of the material is shown in Table 1.

Table 1. Chemical composition wt.% of the Ti-5553 alloy used in this study

Material	O	N	Al	V	Mo	Cr	Fe	Ti
Ti5553	0.14	<0.01	5.03	5.10	5.06	2.64	0.38	Bal.

2.2. Welding Procedures

Autogeneous (no filler metal added) full penetration butt welding joints Ti5553 were obtained by LBW, EBW and GTAW. The welding conditions were as follows.

1. LBW: the weld joints were performed using an Nd:YAG welding machine under a continuous flow of argon (as shielding gas) of 20L/min, a laser power of 2kW with welding speed of 15 mm/sec.
2. EBW: the weld joints were made in the down-hand position using 150kV welding voltage, a traverse speed of 8.5mm/s and welding currents of around 3mA. The details have been reported by Mitchell et al. (2011) and Sabol et al. (2012).
3. GTAW: the weld joints were obtained with a DCEN 50Amp current, a voltage of 10V and with a flow of argon (shielding gas) of 12-16 L/min.

Regardless of the welding procedure, the sizes of samples were always 50x50x1.6mm. Before welding, the samples were cleaned according to ASTM B 600-91 standard. The welding direction was perpendicular to rolling direction (Figure 1).

2.3. Metallography

Metallographic samples for grain structure investigation and for hardness tests were prepared from the welded sheets (as shown in Figure 1). The metallography preparation steps consisted of grinding from 120 grit to 2400 grit SiC paper, polishing to 0.3 μm colloidal alumina, followed by final polishing with 0.05 μm colloidal silica suspension. The samples were etched with Kroll's reagent with a composition of 100 mL water + 2 mL HF + 5 mL HNO_3. An optical microscope was used to characterize the microstructures of the welds.

2.4. Mechanical Testing

Hardness tests on the metallographically-prepared samples were conducted across the weld to produce the hardness profiles. The load used was 300g (HV_{300g}). Tensile tests samples were taken from the welded sheets (Figure 1) in accordance with ASTM E 8M – 04, with the weld located perpendicular to the tensile axis. The tensile tests were conducted at room temperature with a crosshead speed of 3 mm/min.

2.5. Fracture Surface Analysis

Following tensile tests, the fracture surfaces were cleaned with an ultrasonic cleaner, and were examined using a Scanning Electron Microscope (SEM) at relatively low and high magnifications.

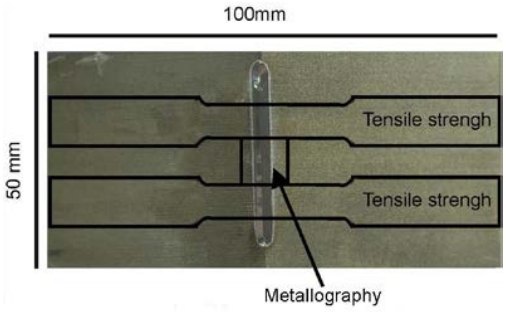

Fig. 1. Schematic diagram indicating the weld joint and locations of samples

3. Results and Discussions

Microstructure of the base metal is given in Figure 2 showing the α/β microstructure where α particles with an average size of less than 5 μm are distributed within the β matrix.

The shapes of the FZ were identical between LBW and EBW, i.e. an hour glass-shaped (Figures 3 and 4), while the GTAW welds showed a V-shaped profile (Figure 5). The presence of hour glass-shaped FZ on the LBW β titanium welds and the absence of this shape in the GTAW has been observed earlier. Liu et al. (1993) and Baeslack et al. (1993b) performed LBW and GTAW, respectively, on a metastable titanium alloy Beta-21S, 1.5 mm thick sheet. Liu et al. (1993) reported a weld zone like hour glass-shaped FZ, while Baeslack et al. (1993b) reported a V-shaped FZ. Odabashi et al. (2010) observed that the hour glass-shaped FZ of LBW Inconel 718 with low amount of heat input, i.e. with high welding speed and power. The explanations on these differences are relatively unclear, although it is believed that the flow of the molten metal and the heat in the molten zone (i.e. later become FZ) are crucial in determining the shape and the size of FZ. According to Rai et al. (2009) the widening top and bottom surface, hence, hour glass-shaped is due to the presence of Marangoni convective currents which drives away the molten metal from the location of heat source. Therefore, the weld pools at the top and bottom surfaces are wide compared to the center of the FZ. Liu et al. (1993) suggested that the hour glass-shaped was due to heat flow in 3D and 2D on the surfaces and the mid-thickness, respectively. In a review by Walsh (2012), it was pointed out that the weld pool geometry is greatly affected by focus/defocus beam which may create a surface tension which is responsible for the metal flow, and hence, the weld zone shape. The V-shaped in the GTAW is conduction dominated where the width of the weld is 2.5x the material thickness.

The widths of the FZ and the HAZ of the GTAW welds were much wider compared with those of LBW and EBW. The FZ created by GTAW was as wide as 5.4 mm compared with 2.6 mm and 1.7 mm made by LBW and EBW, respectively. The HAZ of the GTAW sample reached 3 mm and up to 800 μm for both LBW and EBW samples. The wider weld zones in the GTAW samples compared with EBW and LBW samples is associated with the high heat input into the workpiece on the GTAW process.

The grain sizes in the FZ for all welds were up to a few hundred microns. In the HAZ, large grains were observed at the near HAZ (along the fusion boundary) of up to 200 μm in the EBW and LBW samples, and up to 600 μm for GTAW samples. The grains became gradually smaller towards the BM. The larger grain sizes in the near HAZ are associated with intermediate peak temperature during welding that facilitates grain growth.

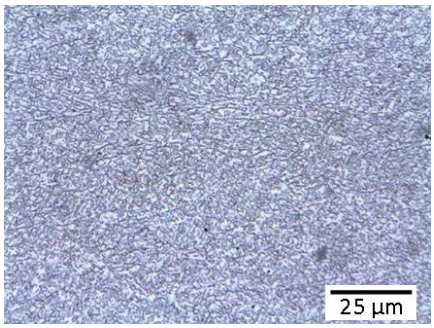

Fig. 2. Microstructure of the base metal showing the α/β microstructure. Note α particles (white).

Some similarities were observed in the weldments' microstructure regardless of the welding method used as described in the followings:

1. The FZ contained a columnar dendritic-typed grain morphology indicating a high concentration of β-stabilizing elements,
2. The HAZ is decorated with retained, equiaxed β grains with larger grains at the fusion boundary and smaller grains towards BM,

3. Epitaxial grain growth from the HAZ into the FZ was clearly observed.

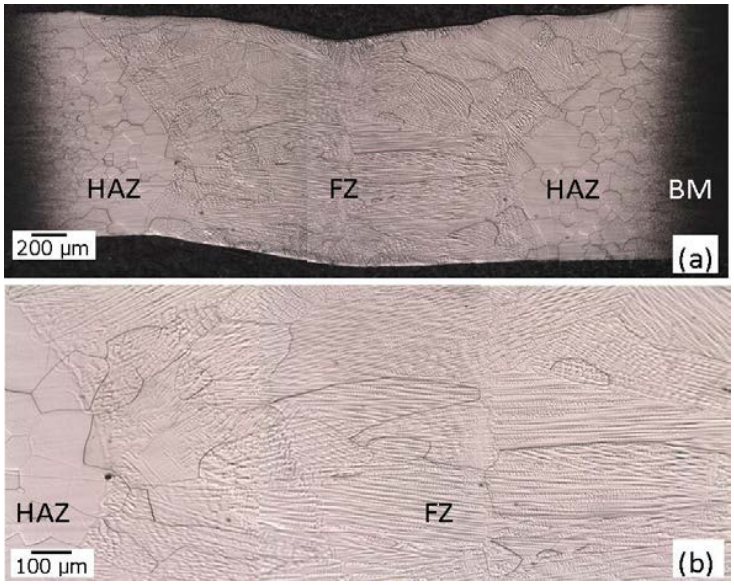

Fig. 3. Weld profile of LBW sample showing the (a) low magnification micrograph of the FZ, HAZ and BM and (b) higher magnification micrograph at the FZ and near HAZ/fusion boundary. Note that the BM is dark due to fast etching rates compared with HAZ and FZ areas

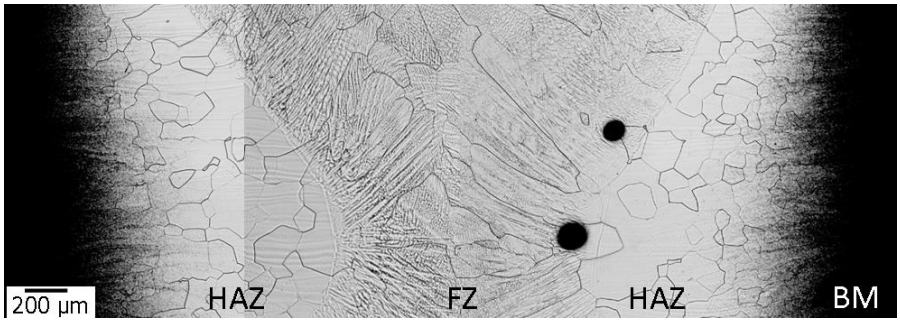

Fig. 4. Weld profile of the EBW samples showing the microstructures in the FZ, HAZ. Note that BM is dark due to fast etching rates compared with HAZ and FZ areas

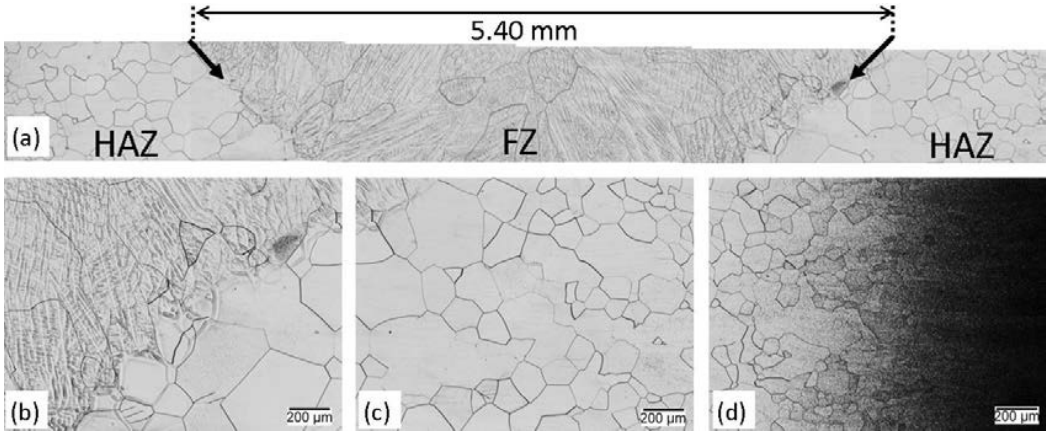

Fig. 5. GTAW weld profile showing the (a) HAZ, FZ and fusion boundary (thick arrows), (b) FZ, fusion boundary and near HAZ, (c) HAZ, and (d) far HAZ and BM. Note that the BM is dark due to fast etching rates compared with HAZ and FZ areas

Hardness profiles for all weldments were similar except for the GTAW weld that has a wider FZ and HAZ due to its wider weld zones. Typical hardness profiles in the as-welded condition are given in Figure 6. Regardless of the welding method used, the hardness values were typically comparable, i.e. 290-320HV in the FZ, 300-360HV in the HAZ and 370-390HV for BM. The weld zones (FZ and HAZ) had lower hardness values compared with that of the base metals. It is noteworthy that the hardness profiles of metastable β titanium alloys are different than those of α or α/β alloys. Hardness values of the α or α/β alloys in the weld zones are generally comparable or higher than that of the BM, due to the formation of α′(alpha prime) or martensite (Amaya-Vazquez et al. 2012). In the metastable β titanium alloy, the formation of these strengthening precipitates is suppressed because of the overwhelming amount of β stabilizing elements leading to a $[Mo]_{eq}$ around 12. According to Bania (1993), α′(alpha prime) or martensite precipitates will not form if the $[Mo]_{eq}$ is greater than 10.

Table 2 summarizes the results obtained from tensile testing. The data showed a reduction in strengths, but the elongation was relatively comparable to that of the un-welded samples.

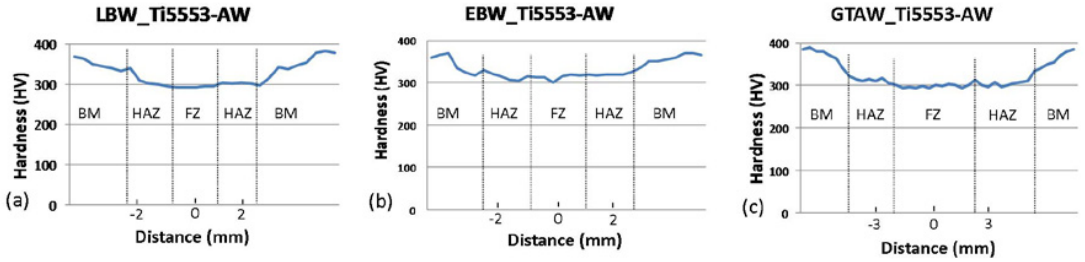

Figure 6. Typical hardness profiles across the weld for (a) LBW, (b) EBW [8] and (c) GTAW/TIG. Note a wider weld zones of GTAW/TIG compared with LBW and EBW.

Table 2. Mechanical properties of Ti5553 on various conditions.

Conditions	YS (MPa)	UTS (MPa)	Elongation (%)	Ref.
Un-welded	1028	1053	12	Mitchell et al. (2011)
As-welded: LBW	N/A	757	9	-
As-welded: EBW	680	680-780	11	Mitchell et al. (2011), Sabol et. al. (2012)
As-welded: GTAW	N/A	591*	N/A	-

*Fractured prematurely

Fracture surfaces from the tensile test samples are given in Figure 7. All samples fractured in the weld zones, and exhibited transgranular fracture modes with microvoid coalescence (dimples) mechanism. This implies that a relatively ductile weld zone results from each of the three welding methods.

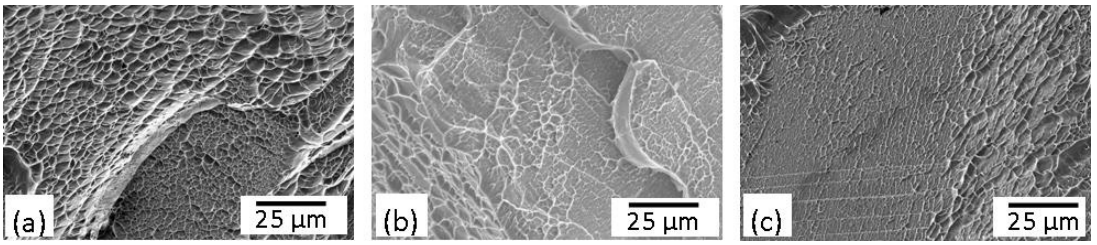

Fig. 7. SEM images showing transgranular fracture with microvoid-coalescence mechanism on (a) LBW, (b) EBW and (c) GTAW.

4. Summary

Ti-5Al-5V-5Mo-3Cr butt welds obtained by LBW, EBW and GTAW have been compared. It has been shown that this new metastable β titanium alloy is weldable. The morphology, the microstructure and the mechanical properties of the welds have been investigated and reported in this paper. The weld profiles due to LBW and EBW showed an hour glass-like appearance, while those from GTAW had a common V-liked shape. From the tensile testing, it is shown that, in the as-welded condition, the strength of the welded specimen is lower than that of the BM (also shown by the lower hardness); however, some ductility was maintained in terms of elongation.

Acknowledgements

The authors (JMSA, MSAV & FJB) would like to thank the financial support of the projects SOLDATIA, Ref. TEP 6180 (Junta de Andalucía, Spain). TP would like to thank The Loewy Family Foundation for sponsoring his research leave at Lehigh University.

References

Amaya-Vazquez, M.R., Sánchez-Amaya, J.M., Boukha, Z., Botana, F.J.. 2012. Microstructure, microhardness and corrosion resistance of remelted TiG2 and Ti6Al4V by a high power diode laser. Corrosion Science Vol. 56, pp. 36-48.

Baeslack III, W.A., Liu, P.S., Barbis, D.P., Schley, J.R., Wood, J.R. 1993 a. Postweld Heat Treatment of GTA Welds in a High-Strength Metastable Titanium Alloy – Beta-C™. Titanium ’92, Science & Tech., F.H. Froes and I. Chaplan (eds), TMS, pp. 1469-1476.

Baeslack III, W.A., Liu P.S. and Paskell T. 1993 b. Weld Solidification and HAZ Liquiation in a Metastable-Beta Titanium Alloy – Beta-21S. Materials Characterization 30, pp.147-54.

Bania P.J., 1993. Beta titanium alloys in the 1990’s. In: Eylon D., Boyer R.R., Koss D.A (Eds.), TMS, Warrendale, PA, pp. 3-14

Becker, D.W., Baeslack III, W.A., 1980. Property-microstructure relationships in metastable-beta titanium alloy weldments. Welding Journal, 59, Research Suppl.,pp. 85s-92s

Donachie Jr, M.J., 2000. Titanium – A Technical Guide, ASM International 2nd edition, pp. 70.

Fanning, J.C., Boyer, R.R. 2003. Properties of TIMETAL 555 – A New Near- Beta Alloy for Airframe Components, Proceedings of the10th World Conference on Titanium, Vol. IV, pp. 2643-2650.

Leyens, C., Peters M. (editors). 2003. Titanium and Titanium Alloys: Fundamentals and Applications. Willey-VCH Verlag GmbH & Co, Weinhamm.

Liu, P.S., Hou, K.H., Baeslack III,W.A., Hurley, J. 1993. Laser Welding of an Oxidation Resistant Metastable-Beta Titanium Alloy – Beta-21S. Titanium ’92 (Froes F.H. and Caplan I, editors), TMS, pp. 1477.

Mitchell, R. Short, A., Pasang, T., Littlefair, G. 2011. Characteristics of Electron Beam Welded Ti and Ti Alloys, Advanced Materials Research Vol. 275, pp. 81-84.

Odabashi, A., Unclu, N., Goller, G., Eruslu, M.N. 2010. A Study on Laser Beam Welding (LBW) Technique: Effect of Heat Input on the Microstructural Evolution of Superalloy Inconel 718. Metall Trans., Vol.41A, pp. 2357-2365.

Rai, R., Burgardt, P., Milewski, J.O., Lienert, T.J., DebRoy, T. 2009. Heat transfer and fluid flow during electron beam welding of 21Cr–6Ni–9Mn Steel and Ti–6Al–4V alloy. J. Phys. D: Appl. Phys. 42**,** pp. 1-12.

Sabol, J.C., Pasang, T., Misiolek, W.Z., Williams, J.C. 2012. Localized tensile strain distribution and metallurgy of electron beam welded Ti–5Al–5V–5Mo–3Cr titanium alloys. Journal of Materials Processing Technology 212, pp. 2380– 2385.

Walsh, C.A. 2012. Laser Welding – Literature Review. Materials Science and Metallurgy Department, University of Cambridge, England.